Exchange catalysis during anaerobic methanotrophy revealed by $^{12}CH_2D_2$ & $^{13}CH_3D$ in methane

Jeanine L. Ash[1*], Matthias Egger[2,#], Tina Treude[3,4], Issaku Kohl[3], Barry Cragg[4], R. John Parkes[4], Caroline P. Slomp[5], Barbara Sherwood Lollar[6], Edward D. Young[3]*

[1]Department of Earth, Environmental and Planetary Sciences, Rice University, Houston Texas, USA

[2]Center for Geomicrobiology, Aarhus University, Aarhus, Denmark

[3]Department of Earth, Planetary, and Space Sciences, UCLA, Los Angeles CA, USA

[4]School of Earth and Ocean Sciences, Cardiff University, Cardiff, UK.

[5]Department of Earth Sciences-Geochemistry, Utrecht University, Utrecht, The Netherlands

[6]Department of Earth Sciences, University of Toronto, Toronto Ontario, Canada

[#]now at The Ocean Cleanup Foundation, Delft, The Netherlands

*correspondence to jeanine.ash@rice.edu, eyoung@epss.ucla.edu

The anaerobic oxidation of methane (AOM) is a crucial component of the methane cycle, but its enzymatic versatility under environmental conditions remains poorly understood. We use sediment samples collected during IODP Expedition 347 to the Baltic Sea to show that relative abundances of $^{12}CH_2D_2$ and $^{13}CH_3D$ molecules in methane gas trace the reversibility of methyl-coenzyme M reductase during AOM by driving methane towards

internal, thermodynamic isotopic equilibrium. These data suggest that $^{12}CH_2D_2$ and $^{13}CH_3D$ together can identify the influence of methanotrophy in environments where conventional bulk isotope ratios are ambiguous, and these findings may lead to new insights regarding the global significance of enzymatic back-flux in the methane cycle.

Recent discoveries of dynamically varying methane in the Martian atmosphere and molecular hydrogen in the plumes of Enceladus have renewed excitement about the role of reduced gases of astrobiological potential and the possibility that habitability may not be unique to Earth (WEBSTER *et al.*, 2015; WAITE *et al.*, 2017). Methane can be produced in a number of biological and abiotic reactions, precluding our ability to determine unequivocally its sources on extraterrestrial bodies (MCCOLLOM AND SEEWALD, 2007; ETIOPE AND SHERWOOD LOLLAR, 2013). Even on Earth, where direct measurements of methane and substrate characteristics are possible, distinguishing microbial from other methanogenesis pathways can be problematic (WHITICAR, 1990; MARTINI *et al.*, 1996; MCCOLLOM AND SEEWALD, 2006; POHLMAN *et al.*, 2009). Additional complexity in sourcing methane is introduced by methanotrophy, the aerobic or anaerobic consumption of methane by microbes. This process can alter parameters that are traditionally useful in sourcing methane such as bulk isotope ratios (WHITICAR, 1999). Perhaps nowhere is this complexity greater than in the deep biosphere, where linking biogeochemistry to metabolisms remains a long-standing challenge compounded by slow rates of reaction (EDWARDS *et al.*, 2012; LAU *et al.*, 2016; MARLOW *et al.*, 2017).

Coupling exploration of enzymatic chemistry that drives these cycles with isotope geochemistry can provide powerful insights. Here, we focus on AOM, estimated to consume ~90% of methane produced in marine sediments (KNITTEL AND BOETIUS, 2009). AOM is traditionally thought to be carried out by a consortium of methane-oxidizing archaea and sulphate-reducing bacteria performing the net reaction $CH_4 + SO_4^{2-} \rightarrow HCO_3^- + HS^- + H_2O$ (BOETIUS *et al.*, 2000). Evidence suggests that these processes can be decoupled (MILUCKA *et al.*, 2012; SCHELLER *et al.*, 2016), and metal oxides may also act as terminal electron acceptors (BEAL *et al.*, 2009). In all cases, the first step of AOM involves interaction between methane and modified methyl-coenzyme M reductase (*mcr*), the terminal enzyme in methanogenesis (KRÜGER *et al.*, 2003; SCHELLER *et al.*, 2010; TIMMERS *et al.*, 2017). Methanogenesis and AOM are linked via this homologous enzyme, prompting questions regarding the reversibility of these metabolisms (LLOYD *et al.*, 2011).

Developments in isotope-ratio mass spectrometry permit the interrogation of these metabolisms by precisely determining concentrations of molecules containing two heavy isotopes, referred to as "clumped" isotopologues. The relative proportions of $^{13}CH_3D$ and $^{12}CH_2D_2$ (reported as $\Delta^{13}CH_3D$ and $\Delta^{12}CH_2D_2$ values relative to a random distribution of isotopes among all CH_4 isotopologues; see Supplementary Information) have known temperature-sensitive equilibrium concentrations and thus are sensitive indicators of reversibility in reactions. Microbial methane displays clumped isotopologue concentrations that range from those consistent with low-temperature equilibration within the environment of formation (INAGAKI *et al.*, 2015) to those with depletions in $\Delta^{13}CH_3D$

and $\Delta^{12}CH_2D_2$ reflecting kinetic processes (WANG *et al.*, 2015; YOUNG *et al.*, 2017). This span in clumped-isotope distributions suggests that enzymatic reactions associated with methanogenesis and methanotrophy are capable of ranging from reversible to kinetic. Previous work using one rare isotopologue ($\Delta^{13}CH_3D$) suggests that that rate of methanogenesis controls the degree of molecular isotopic equilibrium (STOLPER *et al.*, 2015; WANG *et al.*, 2015).

Here, we test the hypothesis that enzymatic-back reaction during AOM drives methane to thermodynamic equilibrium by measuring the isotopic composition of sedimentary methane from Bornholm Basin (Baltic Sea), where methane produced in sediments deposited under brackish-marine conditions diffuses down into lacustrine sediments (see Supplementary Information). Metagenomic analyses reveal that anaerobic methanotrophs (ANME-1) and relatives of the methanogen *Methanohalobium evestigatum* are present, and methyl coenzyme reductase subunit A (*mcr*A) exists throughout the interval (MARSHALL *et al.*, 2017). We compare these data to geochemical profiles (ANDRÉN *et al.*, 2015; EGGER *et al.*, 2017) and present-day rates of methanogenesis and methanotrophy calculated with a multicomponent diagenetic model (DIJKSTRA *et al.*, 2018) to determine parameters controlling the isotopic composition of methane.

Methane concentrations decrease from 10.1 to 1.4 mM over 3.5 to 30.0 meters composite depth [MCD, akin to meters below seafloor (ANDRÉN *et al.*, 2015)] and sulphate concentrations are <0.5 mM throughout the profile. Two sulphate methane transition zones (SMTZ) are noted at 3.3 MCD and 19 MCD (Fig. 1A-B). In sediments that are

sulphate poor but rich in iron oxides (*e.g.* 10-20 MCD [Fig 1C]), metal oxides may play a role in methane consumption (SIVAN *et al.*, 2011). At 3.3 MCD, methane $\delta^{13}C$ is -76.16‰, then increases to a maximum of -71.81‰ by 8.1 MCD, followed by a decrease downcore to -75.59‰ (Fig. 1G). Methane δD at 3.3 MCD is the most negative hydrogen isotope value throughout the core at -244.0‰ and downcore, δD in methane increases to -238.2‰ with a small reversal present between 10-12 MCD before the trend of increasing δD resumes (Fig 1H). In contrast, $\Delta^{13}CH_3D$ and $\Delta^{12}CH_2D_2$ values show trends of consistent increase downcore (Fig. 1E-F). At the shallowest measured depth of 3.5 MCD, values of 4.7‰ and 7.9‰ for $\Delta^{13}CH_3D$ and $\Delta^{12}CH_2D_2$, respectively, are lower than predicted equilibrium values of 6.3‰ and 22.3‰, respectively, for the average subsurface temperature over this interval of 7.8±0.6°C. Activity measurements imply that methanogenesis rates decrease with depth (Table S1). Modelling based on porewater and solid phase profiles shows a methane production peak at 2.7 MCD that decreases downcore and peak Fe-AOM consumption at 12 MCD [Fig. 1D]. The SMTZ at 19 MCD is an additional methane sink not considered in the model by Dijkstra et al., (2018). Therefore, we consider the present-day Fe-AOM rates derived from modelling as a most conservative possible estimate for total AOM activity at these depths.

Comparing the measured $\Delta^{12}CH_2D_2$ values to the equilibrium $\Delta^{12}CH_2D_2$ values associated with measured $\Delta^{13}CH_3D$ values provides a novel parameter capable of demonstrating the degree of thermodynamic disequilibrium for a methane system. $\xi_{^{12}CH_2D_2}$ is analogous to the symbol for the reaction progress variable ($\xi_{^{12}CH_2D_2} = \Delta^{12}CH_2D_{2,\ measured} - \Delta^{12}CH_2D_{2,}$

$_{equilibrium,}$ see Supplementary Information). Values for $\xi_{^{12}CH_2D_2}$ in upper sediments as low as -7.5‰ are clear evidence for disequilibrium, while 0‰ (*i.e.* thermodynamic equilibrium) is approached with increasing depth (Fig. 2). In order to determine how methanogenesis and methanotrophy influence this transition, we discuss evidence for reversibility in each metabolism.

Methanogenesis in intra-species, thermodynamic equilibrium requires reversibility at the final hydrogen-addition step. If methanogenesis is reversible at this terminal step, then its directionality should be influenced by concentrations of products and reactants. For example, in the net reaction $CO_2+4H_2 \rightarrow CH_4+2H_2O$, H_2 concentrations would control the rate of CH_4 oxidation via the reverse reaction, trace methane oxidation (TMO). TMO does occur during methanogenesis, but altering the concentration of H_2 or terminal electron acceptors necessary for oxidizing methane does not increase TMO and has never been shown to consume greater than 0.5% of the CH_4 produced (MORAN *et al.*, 2005). Although some of the first steps of methanogenesis may be reversible (VALENTINE *et al.*, 2004), the final transfer of the methyl group to coenzyme M and the subsequent final hydrogen addition are believed to be irreversible (GÄRTNER *et al.*, 1994; THAUER, 2011). Moreover, with one exception, all clumped-isotope measurements of methane produced by axenic lab cultures have shown methane in intra-species isotopic disequilibrium (STOLPER *et al.*, 2015; WANG *et al.*, 2015; YOUNG *et al.*, 2017), indicating terminal irreversibility in this metabolism. A thermophilic methanogen grown on an H_2/CO_2 substrate produced methane with a clumped isotope temperature consistent with its growth conditions (STOLPER *et al.*, 2014), but this result has yet to be reproduced.

On the other hand, AOM has been shown to have an enzymatic back reaction that suggests the first step of anaerobic methanotrophy is partially reversible, providing a potential mechanism for equilibrating methane isotopologues with environmental temperatures. This back reaction is sensitive to concentrations of the terminal electron acceptor SO_4^{2-} (HOLLER *et al.*, 2011; YOSHINAGA *et al.*, 2014). At high concentrations of SO_4^{2-}, the back reaction produces 3-7% of the CH_4 consumed by AOM, and at low concentrations of SO_4^{2-} (below 0.5 mM), back reaction can produce as much as 78% of the CH_4 consumed by AOM (TIMMERS *et al.*, 2017). Intracellular exposure of methane to *mcr* can lead to isotope exchange catalysis during bond rupture and reformation, and methane that diffuses back out of the cell could move a reservoir towards thermodynamic equilibrium. Using estimates of AOM rates from Dijkstra et al., (2018), we calculate the timescale of this equilibration (see Supplemental Information) to be on the order of 10^3-10^4 years, consistent with the estimated age of methane at 20 MCD of <~8000 years [Fig. S1-S2]. Such timescales would vary in environments with differing rates of AOM.

Conventional isotopic experiments suggest that AOM back-flux is capable of reversing the canonical stable isotope trend expected during methanotrophy (YOSHINAGA *et al.*, 2014); during lab incubations where sulphate is limiting, the methane residue is progressively depleted in heavy isotopes of carbon rather than enriched. Such a reversal is present in the $\delta^{13}C_{CH_4}$ profile of the downward diffusing methane of Bornholm Basin, but interpreting such signals can be difficult where methane produced in modern-late Holocene brackish-marine sediments is transported into glacial-lacustrine sediments with each sedimentary package having unique carbon and hydrogen reservoirs (EGGER *et al.*,

2017). Our findings suggest that when terminal electron acceptors are limiting, equilibrium bond ordering may be used to identify AOM activity even when the bulk isotopic composition of reservoir material is changing and ambiguous. Methane from Kidd Creek Mine (Ontario, Canada) also shows methane isotopologues transitioning with time from non-equilibrated to equilibrated (Fig. 3), suggesting that as energy-rich fractures open, AOM consumes the abiotically produced methane and drives it towards thermodynamic equilibrium (YOUNG *et al.*, 2017).

Methane driven to equilibrium by AOM has a distinct $\Delta^{13}CH_3D$ and $\Delta^{12}CH_2D_2$ composition when compared to methane produced through other known mechanisms (thermogenesis, microbial methanogenesis and abiotic methanogenesis) (Fig. 3). AOM metabolisms have been shown to be active from -1°C to 70°C (NIEMANN *et al.*, 2006; HOLLER *et al.*, 2011), a range of temperatures that is unique and distinguishable from equilibrated thermogenic methane forming in the 100°C to 250°C gas window. Abiotic methane may form also form at low temperatures, yet even when it is apparently equilibrated in $\Delta^{13}CH_3D$, it may exhibit large depletions in $\Delta^{12}CH_2D_2$ that distinguish it from methane that has undergone exchange catalysis during AOM. We suggest that when combined, $\Delta^{12}CH_2D_2$ and $\Delta^{13}CH_3D$ values are sensitive indicators of the degree of thermodynamic equilibrium that may be useful in determining the role of enzymatic back-flux during AOM in the global methane cycle.

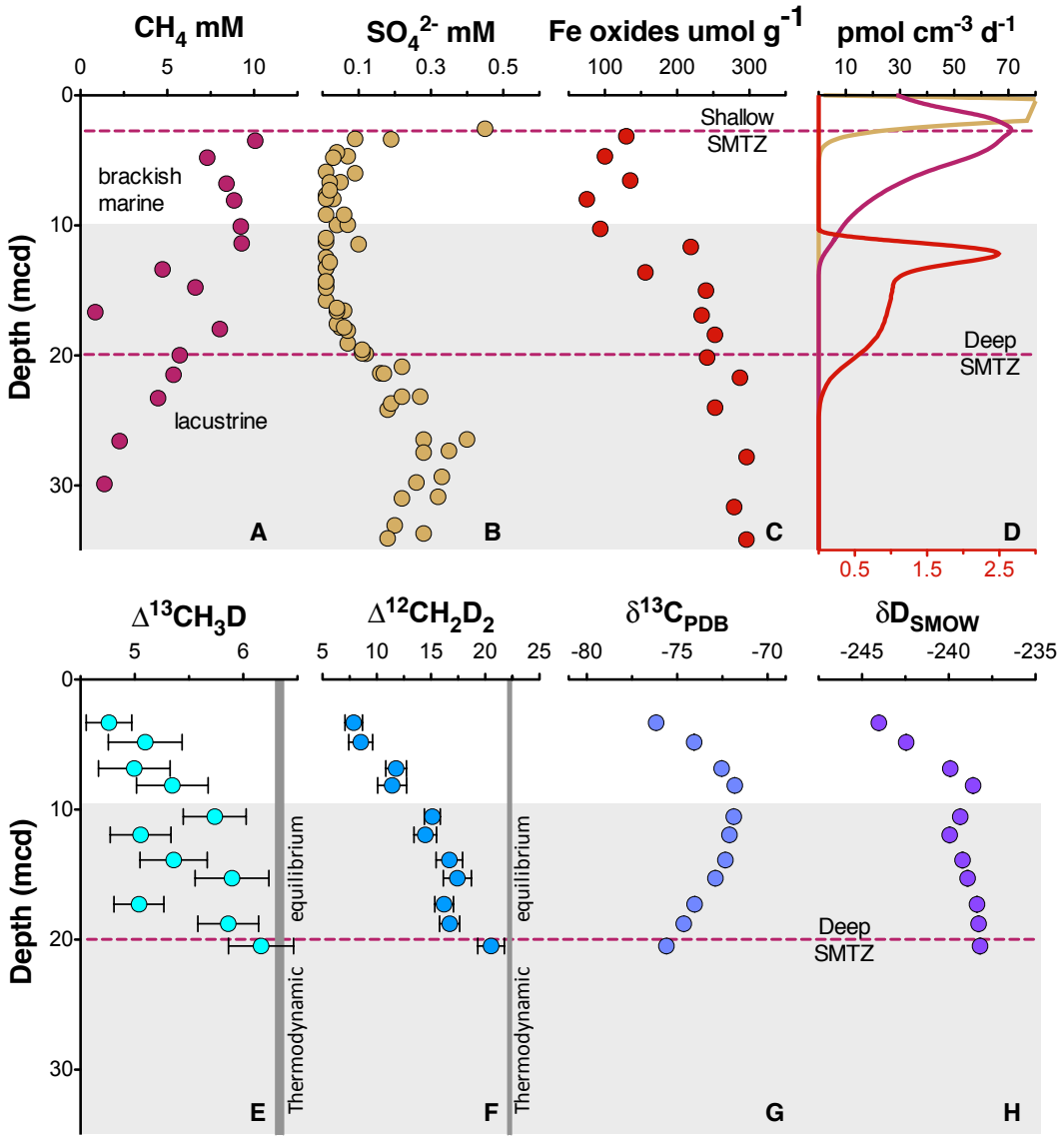

Figure 1: Geochemical profiles (±1σ) from Bornholm Basin from 3-35 MCD. Horizontal grey bar denotes sediments deposited during lacustrine conditions overlain with sediments deposited during brackish marine conditions. Samples were not recovered above the shallow SMTZ. Pink dashed lines denote the shallow (3.3 MCD) and deep (19.8 MCD) SMTZ; only the shallow SMTZ is shown in the bottom panel for clarity. Dark grey vertical bars in **E** and **F** denote equilibrium isotopologue compositions for the

subsurface temperature of 7.8 ± 0.6°C. Modelled CH_4 production, Fe-AOM and SO_4-AOM rates are shown in panel **D** (DIJKSTRA *et al.*, 2018). CH_4 production (purple) and SO_4-AOM (gold) rates correspond with the upper x-axis and Fe-AOM rates (red) correspond with the lower x-axis. SO_4-AOM rates above the upper SMTZ are calculated using bottom-water SO_4 concentrations of 15.0 mmol.

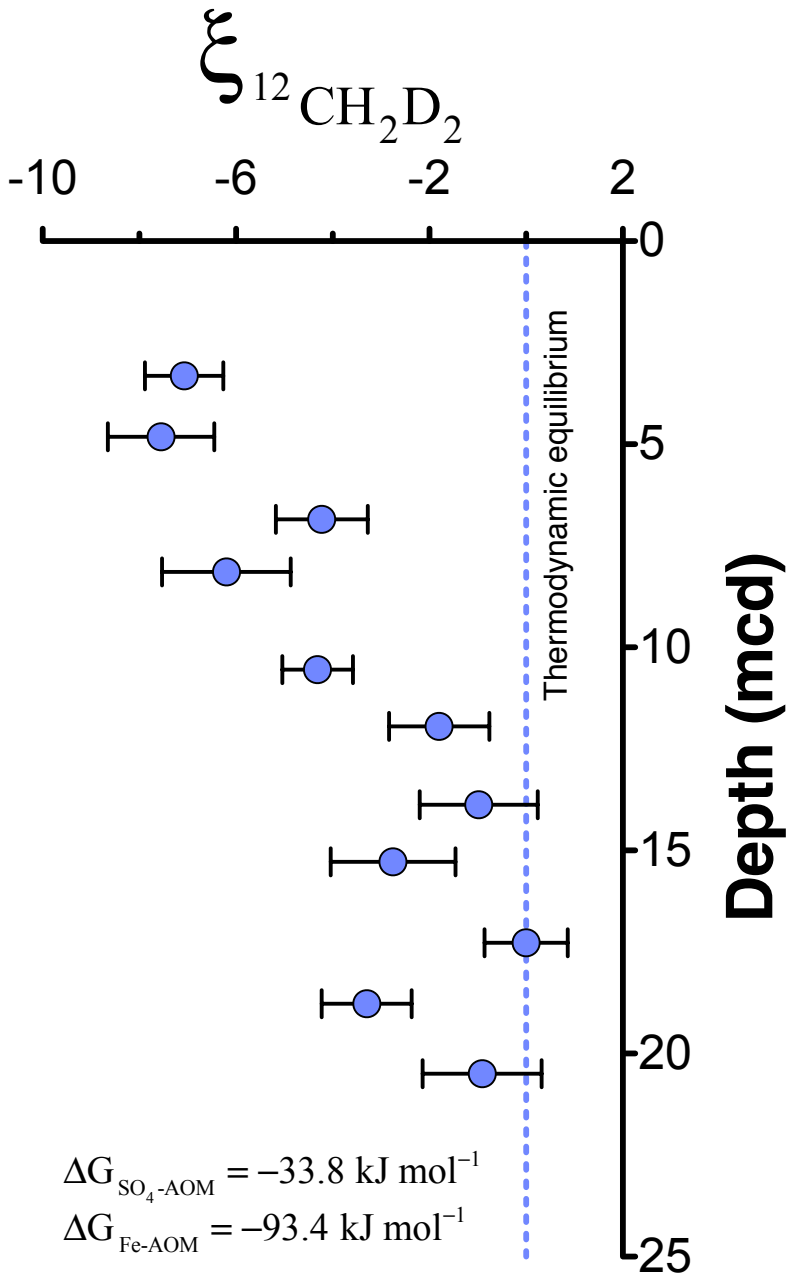

Figure 2: $\xi_{^{12}CH_2D_2}$ values (±1σ) are the most negative at shallow MCD, indicating the greatest departure from equilibrium and approach zero (violet dashed line) with increasing MCD, indicating an approach towards intra-species thermodynamic equilibrium. ΔG values suggest either metabolism is capable of reversibility (See Supplemental Information).

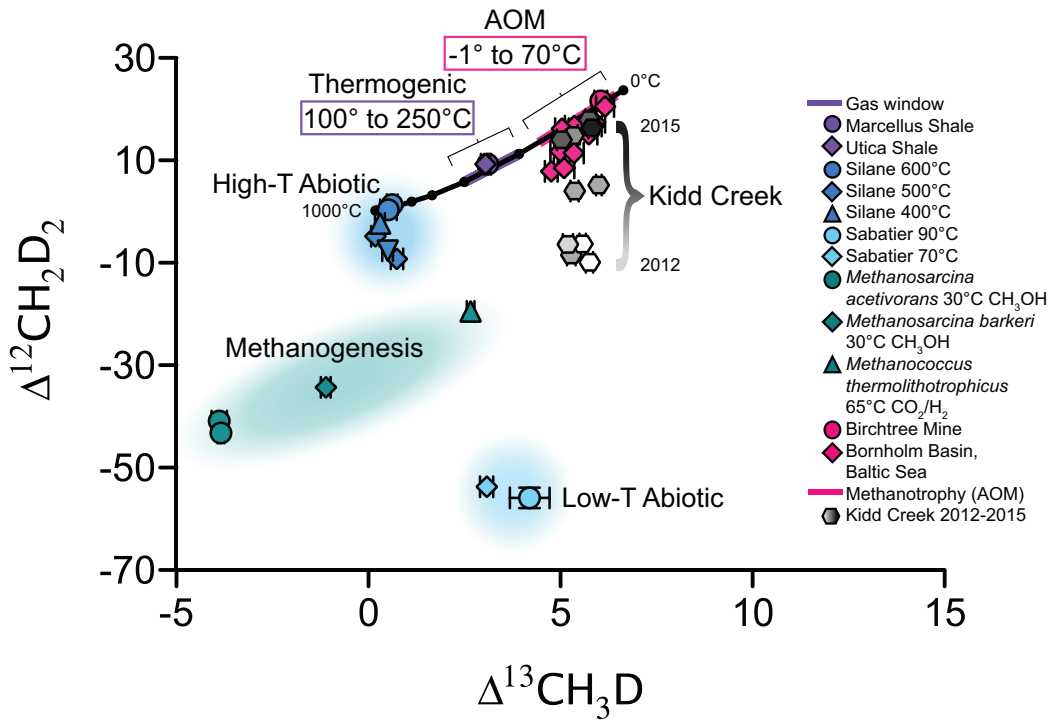

Figure 3: $\Delta^{12}CH_2D_2$ is plotted versus $\Delta^{13}CH_3D$. The solid black line represents theoretical thermodynamic equilibrium abundances (with dots representing 100°C increments from 0-1000°C). Methane produced by thermogenesis, high-temperature abiotic reactions, microbial methanogenesis and low-temperature abiotic reactions inhabit unique zones in double-isotopologue space. AOM, equilibrating through exchange catalysis during enzymatic back reaction, also inhibits a unique zone: low-temperature intra-species thermodynamic equilibrium. Bornholm Basin data (magenta diamonds) span between the methanogenesis and AOM zones, while data (YOUNG *et al.*, 2017) from Kidd Creek Mine (black to white symbols) span from the abiotic to AOM zone.

References

Andrén, T., Jorgensen, B., Cotterill, C., Green, S., Andrén, E., Ash, J., Bauersachs, T., Cragg, B., Fanget, A., Fehr, A. (2015) Expedition 347 Baltic Sea Paleoenvironment. *Proceedings of the Integrated Ocean Drilling Program* 347, 1-66.

Beal, E.J., House, C.H., Orphan, V.J. (2009) Manganese-and iron-dependent marine methane oxidation. *Science* 325, 184-187.

Boetius, A., Ravenschlag, K., Schubert, C.J., Rickert, D., Widdel, F., Gieseke, A., Amann, R., Jørgensen, B.B., Witte, U., Pfannkuche, O. (2000) A marine microbial consortium apparently mediating anaerobic oxidation of methane. *Nature* 407, 623-626.

Dijkstra, N., Hagens, M., Egger, M., Slomp, C.P. (2018) Post-depositional vivianite formation alters sediment phosphorus records. *Biogeosciences* 15, 861-883.

Edwards, K.J., Becker, K., Colwell, F. (2012) The deep, dark energy biosphere: intraterrestrial life on earth. *Annual Review of Earth and Planetary Sciences* 40, 551-568.

Egger, M., Hagens, M., Sapart, C.J., Dijkstra, N., van Helmond, N.A., Mogollón, J.M., Risgaard-Petersen, N., van der Veen, C., Kasten, S., Riedinger, N. (2017) Iron oxide reduction in methane-rich deep Baltic Sea sediments. *Geochimica Et Cosmochimica Acta* 207, 256-276.

Etiope, G., Sherwood Lollar, B. (2013) Abiotic Methane on Earth. *Reviews of Geophysics* 51, 276-299.

Gärtner, P., Weiss, D.S., Harms, U., Thauer, R.K. (1994) N5‐Methyltetrahydromethanopterin: Coenzyme M Methyltransferase from Methanobacterium thermoautotrophicum. *The FEBS Journal* 226, 465-472.

Holler, T., Wegener, G., Niemann, H., Deusner, C., Ferdelman, T.G., Boetius, A., Brunner, B., Widdel, F. (2011) Carbon and sulfur back flux during anaerobic microbial oxidation of methane and coupled sulfate reduction. *Proceedings of the National Academy of Sciences* 108, E1484-E1490.

Inagaki, F., Hinrichs, K.-U., Kubo, Y., Bowles, M.W., Heuer, V.B., Hong, W.-L., Hoshino, T., Ijiri, A., Imachi, H., Ito, M. (2015) Exploring deep microbial life in coal-bearing sediment down to~ 2.5 km below the ocean floor. *Science* 349, 420-424.

Knittel, K., Boetius, A. (2009) Anaerobic oxidation of methane: progress with an unknown process. *Annual review of microbiology* 63, 311-334.

Krüger, M., Meyerdierks, A., Glöckner, F.O., Amann, R., Widdel, F., Kube, M., Reinhardt, R., Kahnt, J., Böcher, R., Thauer, R.K. (2003) A conspicuous nickel protein in microbial mats that oxidize methane anaerobically. *Nature* 426, 878-881.

Lau, M.C.Y., Kieft, T.L., Kulouo, O., Linage-Alvarez, B., van Heerden, E., Lindsay, M.R., Magnabosco, C., Wang, W., Wiggins, J.B., Guo, L., Perlman, D.H., Kyin, S., Wei, S., Li, L., Sherwood Lollar, B., Onstott, T. (2016) An oligotrophic deep-subsurface community dependent on syntrophy is dominated by sulfur-driven autotrophic denitrifiers. *Proceedings of the National Academy of Sciences* 113, E7927-E7936.

Lloyd, K.G., Alperin, M.J., Teske, A. (2011) Environmental evidence for net methane production and oxidation in putative ANaerobic MEthanotrophic (ANME) archaea. *Environmental Microbiology* 13, 2548-2564.

Marlow, J.J., Steele, J.A., Ziebis, W., Sheller, S., Case, D., Reynard, L.M., Orphan, V.J. (2017) Monodeuterated Methane, an Isotopic Tool To Assess Biological Metabolism Rates. *mSphere* 2, e00309-17.

Marshall, I.P., Karst, S.M., Nielsen, P.H., Jørgensen, B.B. (2017) Metagenomes from deep Baltic Sea sediments reveal how past and present environmental conditions determine microbial community composition. *Marine genomics*.

Martini, A.M., Budai, J.M., Walter, L.M., Schoell, M. (1996) Microbial generation of economic accumulations of methane within a shallow organic-rich shale. *Nature* 383, 155-158.

McCollom, T.M., Seewald, J.S. (2006) Carbon isotope composition of organic compounds produced by abiotic synthesis under hydrothermal conditions. *Earth and Planetary Science Letters* 243, 74-84.

McCollom, T.M., Seewald, J.S. (2007) Abiotic synthesis of organic compounds in deep-sea hydrothermal environments. *Chemical Reviews* 107, 382-401.

Milucka, J., Ferdelman, T.G., Polerecky, L., Franzke, D., Wegener, G., Schmid, M., Lieberwirth, I., Wagner, M., Widdel, F., Kuypers, M.M. (2012) Zero-valent sulphur is a key intermediate in marine methane oxidation. *Nature* 491, 541-546.

Moran, J.J., House, C.H., Freeman, K.H., Ferry, J.G. (2005) Trace methane oxidation studied in several Euryarchaeota under diverse conditions. *Archaea* 1, 303-309.

Niemann, H., Lösekann, T., De Beer, D., Elvert, M., Nadalig, T., Knittel, K., Amann, R., Sauter, E.J., Schlüter, M., Klages, M. (2006) Novel microbial communities of the Haakon Mosby mud volcano and their role as a methane sink. *Nature* 443, 854-858.

Pohlman, J., Kaneko, M., Heuer, V., Coffin, R., Whiticar, M. (2009) Methane sources and production in the northern Cascadia margin gas hydrate system. *Earth and Planetary Science Letters* 287, 504-512.

Scheller, S., Goenrich, M., Boecher, R., Thauer, R.K., Jaun, B. (2010) The key nickel enzyme of methanogenesis catalyses the anaerobic oxidation of methane. *Nature* 465, 606.

Scheller, S., Yu, H., Chadwick, G.L., McGlynn, S.E., Orphan, V.J. (2016) Artificial electron acceptors decouple archaeal methane oxidation from sulfate reduction. *Science* 351, 703-707.

Sivan, O., Adler, M., Pearson, A., Gelman, F., Bar-Or, I., John, S.G., Eckert, W. (2011) Geochemical evidence for iron‐mediated anaerobic oxidation of methane. *Limnology and Oceanography* 56, 1536-1544.

Stolper, D.A., Martini, A.M., Clog, M., Douglas, P.M., Shusta, S.S., Valentine, D.L., Sessions, A.L., Eiler, J.M. (2015) Distinguishing and understanding thermogenic and biogenic sources of methane using multiply substituted isotopologues. *Geochimica Et Cosmochimica Acta* 161, 219-247.

Stolper, D.A., Sessions, A.L., Ferreira, A.A., Neto, E.V.S., Schimmelmann, A., Shusta, S.S., Valentine, D.L., Eiler, J.M. (2014) Combined ^{13}C-D and D-D clumping in methane: Methods and preliminary results. *Geochimica Et Cosmochimica Acta* 126, 169-191.

Thauer, R.K. (2011) Anaerobic oxidation of methane with sulfate: on the reversibility of the reactions that are catalyzed by enzymes also involved in methanogenesis from CO_2. *Current Opinion in Microbiology* 14, 292-299.

Timmers, P.H., Welte, C.U., Koehorst, J.J., Plugge, C.M., Jetten, M.S., Stams, A.J. (2017) Reverse Methanogenesis and respiration in methanotrophic archaea. *Archaea* 2017.

Valentine, D.L., Chidthaisong, A., Rice, A., Reeburgh, W.S., Tyler, S.C. (2004) Carbon and hydrogen isotope fractionation by moderately thermophilic methanogens. *Geochimica Et Cosmochimica Acta* 68, 1571-1590.

Waite, J.H., Glein, C.R., Perryman, R.S., Teolis, B.D., Magee, B.A., Miller, G., Grimes, J., Perry, M.E., Miller, K.E., Bouquet, A. (2017) Cassini finds molecular hydrogen in the Enceladus plume: Evidence for hydrothermal processes. *Science* 356, 155-159.

Wang, D.T., Gruen, D.S., Lollar, B.S., Hinrichs, K.-U., Stewart, L.C., Holden, J.F., Hristov, A.N., Pohlman, J.W., Morrill, P.L., Könneke, M. (2015) Nonequilibrium clumped isotope signals in microbial methane. *Science* 348, 428-431.

Webster, C.R., Mahaffy, P.R., Atreya, S.K., Flesch, G.J., Mischna, M.A., Meslin, P.-Y., Farley, K.A., Conrad, P.G., Christensen, L.E., Pavlov, A.A. (2015) Mars methane detection and variability at Gale crater. *Science* 347, 415-417.

Whiticar, M.J. (1990) A geochemial perspective of natural gas and atmospheric methane. *Organic Geochemistry* 16, 531-547.

Whiticar, M.J. (1999) Carbon and hydrogen isotope systematics of bacterial formation and oxidation of methane. *Chemical Geology* 161, 291-314.

Yoshinaga, M.Y., Holler, T., Goldhammer, T., Wegener, G., Pohlman, J.W., Brunner, B., Kuypers, M.M.M., Hinrichs, K.U., Elvert, M. (2014) Carbon isotope equilibration during sulphate-limited anaerobic oxidation of methane. *Nature Geoscience* 7, 190-194.

Young, E., Kohl, I., Lollar, B.S., Etiope, G., Rumble, D., Li, S., Haghnegahdar, M., Schauble, E., McCain, K., Foustoukos, D. (2017) The relative abundances of resolved $^{12}CH_2D_2$ and $^{13}CH_3D$ and mechanisms controlling isotopic bond ordering in abiotic and biotic methane gases. *Geochimica Et Cosmochimica Acta* 203, 235-264.